Journal of New Materials for Electrochemical Systems 17, 071-075 (2014)

Effective Electro-Fenton Degradation of Reactive Black 5 Dye using Modified Electrode with Cu-Zeolites

Miguel A. Oliver-Tolentino[1,†], Elmer Jiménez-Álvarez[1], María de Jesús Martínez-Ortiz[1], Efrén García-Báez[2], M.Olivia Franco-Hernández[2] and Ariel Guzmán-Vargas[1,*]

[1]Instituto Politécnico Nacional, ESIQIE, Departamento de Ingeniería Química - Laboratorio de Investigación en Materiales Porosos, Catálisis Ambiental y Química Fina, UPALM Edif.7 P.B. Zacatenco, GAM, México, D.F. 07738, México
[2]Instituto Politécnico Nacional, UPIBI, Departamento de Ciencias Básicas, Av. Acueducto s/n, Barrio La Laguna, Col. Ticomán, GAM, México, D.F. , 07340, México

Received: December 10, 2013, Accepted: February 08, 2014, Available online: April 15, 2014

Abstract: *The electrocatalytic production of hydroxyl radical (HO•) on the surface of zeolite modified electrode (ME) employing Cu-Zeolites (ZSM5 and β) with different theoretical ionic exchange (15 and 100%) was investigated (ME/Cu-Zeolites). The i-E characteristic of ME/Cu-ZSM-5 presented the faradic process associated to redox couple Cu^{2+}/Cu^{+}. On the other hand, voltammetric studies showed that in presence of H_2O_2, the cathodic peak current of ME/Cu-Zeolites increases followed by a decrease in the corresponding anodic current. This suggested that hydroxyl radical was produced by a cooperative effect of the acidic properties of zeolite and copper that acts as a redox mediator on the electrode surface via an electrocatalytic mechanism. Experiments of degradation using azo dye Reactive Black 5 as probe molecule exhibited that the concentration of azo dye decreased in the time, this confirms the formation of hydroxyl radical on the surface of modified electrode; kinetics parameters demonstrated that the ME/Cu- β with 15% of ionic exchange presented the highest catalytic activity.*

Keywords: Hydroxyl radical, electrocatalysis, chemical oxygen demand, Cu-Zeolite, Reactive Black 5

1. INTRODUCTION

Azo dyes represent the largest class of textile dyes in industrial use. This extensive use of reactive dyes has a strong impact especially on aquatic ecosystems, leading to their imbalance. This kind of synthetic dyes are generally resistant to oxidative biodegradation since they are designed to exhibit high resistance to fading caused by chemical, biological and light-induced oxidation, consequently they are hard to be removed from wastewater [1].

At present, it is commonly known that most of these dyes and their intermediates possess carcinogenic potential which brings serious consequences to the environment. In many developed countries, textile wastewater contaminated with these dyes is directly discharged without treatment to rivers, lakes or the ocean [2,3]. In this area, the complete mineralization of organic pollutants is the most suitable way to diminish the environmental impact. For this reason, a priority over the last few years is based on the development and the evaluation of some advanced oxidation processes (AOPs), characterized by the hydroxyl radicals generation, which are highly reactive and non-selective oxidants [4,5]. Hydroxyl radicals (HO•), highly reactive species generated in sufficient quantities by these systems, have the ability to oxidize the majority of organics in industrial effluents [6]. Common AOPs involve Fenton and photo-Fenton processes, ozonation, electrochemical oxidation, photolysis with H_2O_2 and O_3, high-voltage electrical discharge process and TiO_2 photocatalysis [7,8]. Fenton-like processes have been used as a powerful source of hydroxyl radicals from H_2O_2 in the presence of iron cations and mild reaction conditions to treat these effluents [9], copper ion also has shown interesting results in the Fenton process [10].

However, homogenous Fenton systems suffer since some well-known limitations like limited pH range (pH 2–4), production of metal ion containing waste sludge, which is difficult to dispose, and catalyst deactivation by some iron complexing agents like phosphates ions. These reasons stimulated the research on heterogeneous Fenton-type catalysts. Heterogeneous catalysis eliminates

To whom correspondence should be addressed:
Email: *aguzmanv@ipn.mx, †otma_iq@hotmail.com

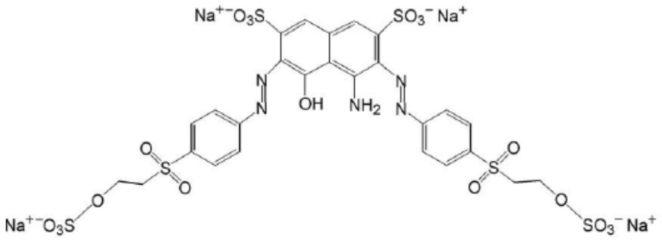

Figure 1. Chemical Structure of RB5

the need of adding soluble catalytic substances and the need of treating the resultant sludge [11]. In this context, the use of zeolites exchanged with transition metal ion has been reported [12-14]. The aim of this work was to study the degradation of reactive black 5 (RB 5), by Fenton processes, producing the hydroxyl radicals from hydrogen peroxide using Cu-Zeolite modified electrode (ZME).

2. EXPERIMENTAL SECTION

2.1. Reactive Black 5 (RB5)

RB 5 (Figure 1), a representative reactive diazo dye typically found in high percentage over other reactive dyes in dye bath effluents, their molecular weight is 991.82 g mol^{-1}, and this compound shows a main absorbance peak around 597 nm.

2.2. Cu-zeolite preparation

Two different kinds of zeolite NH_4-ZSM5 and NH_4-β with Si/Al ratio=15 were employed (Zeolyst CBV2024 and CBV3487). The Cu(x)-Zeolite(x = 200 x Cu/Al, mol/mol) was prepared by ion-exchange method with 15% and 100% of theoretical exchange; the materials were labeled as Cu(x)-zeolite, where the x = theoretical exchange percentage and zeolite is the kind of solid used. Briefly, 2 g NH_4-Zeolite were added to 500 cm^3 of $Cu(NO_3)_2 \cdot 7H_2O$ aqueous solution and stirred during 24 h at room temperature. Then, the solid was filtered, washed three times with de-ionized water and dried at 353 K in air atmosphere.

2.3. Working Electrode Preparation

A polymer solution was obtained by mixing 3 mg of poly-(methacrylic acid methyl ester), PMMA, (Aldrich, USA) in 1 mL of methyl acrylate, MA, (Aldrich, USA). 0.2 g of Cu(x)-Zeolite or NH_4-Zeolite was added in this solution. The mixture was homogeneously dispersed by an ultrasound bath for 30 min. Then, 0.5 μL of the resulting suspension were deposited at the surface of glassy carbon electrode (diameter = 5 mm) and dried with argon at room temperature. The obtained zeolite modified electrodes (ZME) were labeled as ME/Cu(x)-Zeolite.

2.4. Electrochemical Measurements

The electrochemical analyses were carried out in a potentiostat-galvanostat VERSASTAT3-400 (Princeton Applied Research). A three-electrode standard electrochemical cell was used for the cyclic voltammetry (CV) measurements at 20 mV s^{-1}. A carbon rod and a calomel (SCE) electrode were used as counter and reference electrode, respectively. Prior to use, the solution was purged with argon for at least 15 min.The initial potential was fixed at open circuit potential toward cathodic direction. 0.1 M NaCl solution was used as supporting electrolyte.

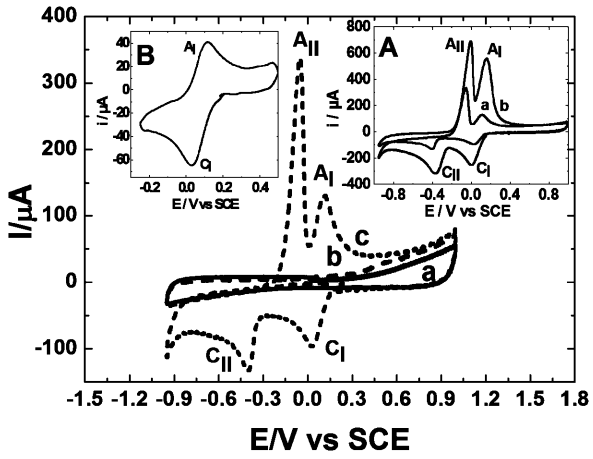

Figure 2. Cyclic Voltammetry of a) UGC, b) NH_4-β, c) Cu(15)-β in NaCl (0.1 $molL^{-1}$) at ν= 20 mV s^{-1}; Inset A: Cyclic Voltammetry of a) Cu(15)-β and b) Cu(100)-β, inset B: Cyclic Voltammetry of Cu(15)-β in a potential window -0.3 at 0.5V/SCE.

2.5. Catalytic Evaluation Tests

Degradation-discoloration tests were carried out in a three-electrode standard electrochemical cell in batch operation, the constant potential (cronoamperometric measurement) was applied using a potentiostate-galvanostate VERSASTAT3-400. The reaction evolution, sampling over the time, was followed by UV-Vis spectroscopy, using a Perkin Elmer Lambda 35 spectrophotometer. Chemical oxygen demand (COD) parameter was measured in a Hacht apparatus employing Hanna kits (HI93754C certified COD reagents).

3. RESULTS AND DISCUSSION

3.1. Electrochemical Behavior of modified electrode with Cu-zeolite

The electrochemical behavior of the as-prepared Cu(x)-zeolite materials was first studied in 0.1M NaCl solution in order to establish the potential range and, in a first approach, the stability of this material. Figure 2 shows the cyclic voltammetry (CV) profile for ME/Cu(15)-β (curve c). This profile has been compared with ME/NH_4-β (curve b) and unmodified mirror finished glassy carbon (UGC, curve a). The potential scan, at 20 mV s^{-1}, started at open circuit potential (OCP) in the cathodic direction. *i-E* characteristics of curves a and b are similar for the two electrodes, where the presence of a small contribution of non-faradic current is evident and it can be associated to the double layer-charge interactions. On the other hand, the profile corresponding to ME/Cu(15)-β, exhibited two cathodic peaks, C_I (c.a.0.03 V/SCE) and C_{II} (c.a. -0.4 V/SCE) and two anodic peaks, A_I (0.11 V/SCE) and A_{II} (-0.05 V/SCE), attributed to copper faradaic processes. This performance are associated to Cu^{2+} reduction via two one-electron steps due to the Cu^+ formation (peak C_I), followed by the reduction to Cu^0 (peak C_{II}). In addition, during the positive potential sweep, the Cu^0 oxidation to Cu^+ (peak A_{II}) and Cu^+ to Cu^{2+} (peak A_I) are evident, near to -0.8V/SCE the hydrogen evolution reaction (HER) takes place, this

electrochemical behavior on this kind of ZME has been reported by our group in previous work [15]. In order to evaluate the effect of copper content on the zeolite, experiments with ME/Cu(100)-β were carried out, and they were compared with experiments obtained by ME/Cu(15)-β (see inset A). Similar electrochemical behavior is presented by ME/Cu(100)-β, but the potential where the faradic processes occur are different, the peak C_I shifts to cathodic potential until 0.005V/SCE; whereas the peaks C_{II}, A_{II} and A_I shifts to anodic potential until -0.36, -0.005 and 0.16V/SCE respectively, the current intensity increase due to the amount of copper present in the zeolite structure framework. On the other hand, the inset B in Figure 1 showed only the peaks A_I and C_I, associated to the electrochemical behavior of Cu^{2+}/Cu^{+} redox couple, which occurs in a potential window between -0.3 to 0.5V/SCE. Similar behavior was observed in the ME/Cu(x)-ZSM5 (Figures not shown).

The peak potential for the reduction of Cu^{2+} to Cu^{+} (Ep_{CI}), potential gradients (ΔEp), anodic current intensity and cathodic relationship (I_a/I_c) values are presented in Table 1. The results exhibited that Cu^{2+}/Cu^{+} redox couple electrochemical process on the ZME is quasi-reversible, where ME/Cu(15)-β electrode exhibited the lowest ΔEp and the highest I_a/I_c.

3.2. ME/Cu-Zeolite electrochemical behavior in presence of hydrogen peroxide (H_2O_2)

Hydrogen peroxide electrochemical reduction on the surface of a glassy carbon electrode (GC) was studied using a NaCl solution (0.1 M), as supporting electrolyte. The results are represented in the inset of Figure 3. The GCi-*E* characteristics in NaCl with and without H_2O_2 are shown in curve b and a, respectively. Any faradic process is evident on GC without H_2O_2 (curve a), whereas in the presence of hydrogen peroxide, it can be observed a faradic current near to -0.2 V/SCE, suggesting the H_2O_2 electrochemical reduction to hydrogen. On the other hand, the ME/Cu(15)-β without H_2O_2 exhibited the faradic process associated to redox couple Cu^{2+}/Cu^{+}as discussed before.

In the presence of H_2O_2, using ME/Cu(15)-β, the current density in the cathodic peak (C_I) was greatly increased over the ordinarily observed just for redox couple Cu^{2+}/Cu^{+}, while the corresponding anodic peak (A_I) was substantially depressed on the reverse cycle (curve d), indicating a chemical redox reaction between hydrogen peroxide and Cu^{+} produced during cathodic scan. This behavior was verified with experiments to different H_2O_2 concentrations, where the cathodic signal increases proportionally to the hydrogen peroxide concentration (Figure not shown).

After the initial electrochemical reduction of Cu^{2+} into Cu^{+}, the proposed mechanism to explain the electrocatalytic behavior can be one of Fenton type [11], using modified electrode with Cu-zeolites [10]:

Table 1. Peak potential, potential differences and current ratio in different electrodes

Electrode	Ep_{CI}/V vs SCE	ΔEp/V	I_a/I_c
ME/Cu(15)-β	0.033	0.079	0.72
ME/Cu(100)-β	0.014	0.107	0.66
ME/Cu(15)-ZSM5	0.057	0.104	0.69
ME/Cu(100)-ZSM5	0.037	0.121	0.64

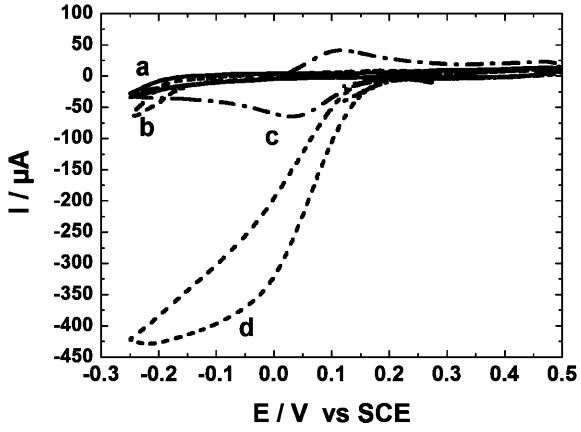

Figure 3. Cyclic Voltammetry of a) and b) UGC, c) and d) ME/Cu(15)-β in NaCl (0.1 molL^{-1}) at ν = 20 mV s^{-1}; a) and c) without H_2O_2 and b) and d) with 3.3 gL^{-1} H_2O_2.

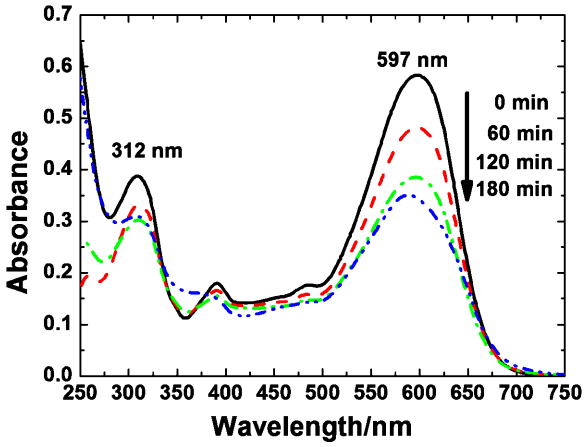

Figure 4. UV-Vis Spectra of RB5 at different degradation reaction time on the surface of ME/Cu(15)-β in NaCl (0.1 molL^{-1}) and 3.3 gL^{-1} H_2O_2 at an applied potential of -0.05 V/SCE.

$$Cu^{+} + H_2O_2 \rightarrow Cu^{2+} + OH\bullet + HO$$

$$Cu^{+} + OH\bullet \rightarrow Cu^{2+} + OH^{-}$$

This mechanism can be proposed due to the required pH condition for Fenton process, i.e, the acidity is provided by zeolite surface as it was demonstrated before [16]. In order to evaluate the electrocatalytic activity toward Fenton process, the enhancement factor (*EF*) was calculated using Eq. (1).

$$EF = (I_{peak} - I_{peakHP})/I_{peakHP} \quad (1)$$

Where I_{peak} is the cathodic current intensity in absence of hydrogen peroxide and I_{peakHP} is the cathodic current in the presence of 3.3 g L^{-1} H_2O_2 for current measurements at-0.1V/SCE. In order to take advantage of oxidizing power of hydroxyl radicals formed in the electrode surface, the RB5 azo dye was used as probe molecule.

3.3. RB5 Degradation

Dye solution (20 mg L^{-1}) was placed in the electrochemical cell,

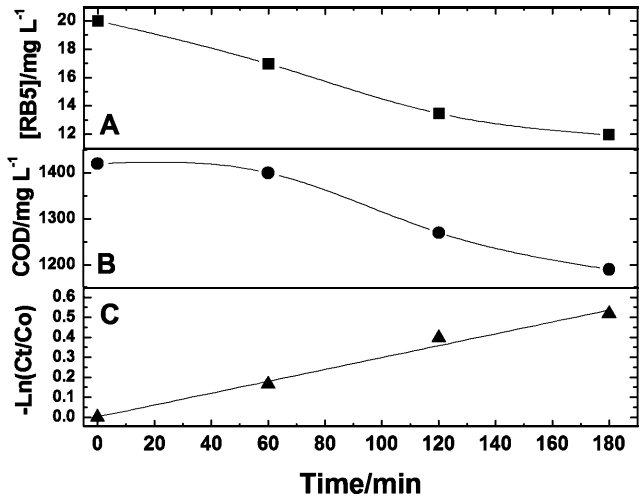

Figure 5. A) Concentration of RB5 in function of reaction time, B) Chemical Oxygen Demand in function of reaction time and C) $-Ln(C_t/C_o)$ vs time for kinetics parameters, the reaction conditions are -0.1V/SCE using 3.3 g L^{-1} of H_2O_2 and NaCl (0.1 molL^{-1}).

using the ME/Cu(15)- β as working electrode in NaCl solution (0.1 mol L^{-1}) as supporting electrolyte and 3.3 g L^{-1} H_2O_2, the applied potential was -0.05 V/SCE. Figure 4 shows temporal changes in the UV-visible spectrum. As it can be clearly seen, RB5 exhibits two characteristic absorbance bands at 598 nm in the visible region and 312 nm in the UV region, both of which progressively disappeared upon applied potential. The band at 598 nm is characteristic for the RB5 chromophore azo double bond, while the band close to 312 nm is associated to aromatic compound present in the molecule; it is evident that the absorbance decreases faster in the band c.a. 598 than in the band c.a. 312 nm.

RB5 concentration decreases as function of time reaching about 40% of discoloration at 180 minutes (Figure 5A). On the other hand, experiments concerning the evolution of chemical oxygen demand were carried out at different times of electrolysis. The results are shown in Figure 5B. During the first hour, any change was observed, but after 60 minutes COD removal began to decrease, until reach 15% of COD removal at 180 min, based on these results, is possible to mineralize the organic compounds until CO_2, due to the high oxidizing power of hydroxyl radical.

In order to study the discoloration kinetics, a pseudo-first order with respect to dye concentration was proposed (Figure 5C). The next model represents the pseudo first order reaction rate.

$$-Ln\,(C_t/C_0) = kt$$

Where C_0 is the initial dye concentration at time = 0, C_t is the dye concentration at different reaction time (t), and k represents the constant rate.

It should be mentioned that the kinetic model proposed is a general approach keeping in mind those others phenomena occuring during the reaction, i.e. HO• radicals consumption due to dye oxidation from electrocatalytic Fenton process, the linear correlation let us calculate some kinetics parameters. In this case, the k value corresponded to 0.00376 min^{-1}.

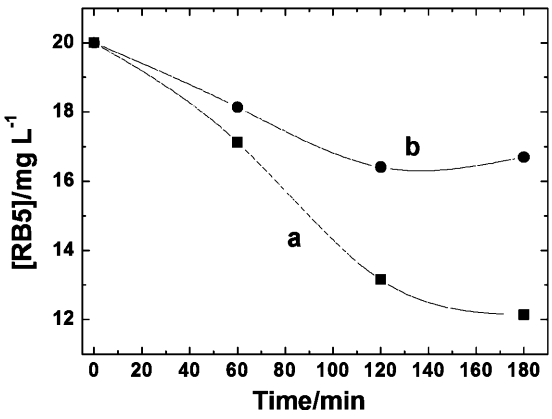

Figure 6. RB5 Concentration in function of reaction time, the reaction conditions at -0.1V/SCE were: 3.3 g L^{-1} of H_2O_2 and a) NaCl(0.1 molL^{-1}) and b) $NaNO_3$ (0.1 molL^{-1}).

Similar experiments were carried out for the others ZME. The results are shown in the Table 2. Where η is the overpotential and EF is the enhancement factor. Based in this results, it is clear that ME/Cu(15)-β exhibited the highest electrocatalytic activity, this can be associated to the widely open porosity of the zeolite β structure [17].

3.4. Electrolyte Effect

In the electrochemical experiments, electrolyte has an important effect over faradic processes. In this context, Figure 6 presents the discoloration reaction as function of time using NaCl (curve a), and $NaNO_3$ (curve b). Under similar conditions, in presence of $NaNO_3$, discoloration decrease. This behavior suggests that chloride ions played an important role, resulting in the RB5 increasing removal in the NaCl medium, attributed to powerful oxidants formation of active chlorine (e.g. HClO and Cl_2) [18], by the interaction between HO• radicals and Cl^- ion because chlorine cannot be absorbed in the modified electrode surface or diffuses into the zeolite framework due to electrostatic repulsion [15]. Once active chlorine is transferred into the bulk solution, this induces a series of reactions and consequently promotes RB5 removal.

3.5. Applied Potential Effect

In order to observe the effect of cathodic potential, experiments were carried out to different applied potentials (Figure 7): before, near and after the potential peak for copper reduction. Before to the potential peak at 0.05 V/SCE (curve c), the discoloration occurs slowly until reach a discoloration efficiency of about 20% after 180 minutes. This behavior is due to the mix between Cu^{2+}/Cu^{+} formed at this potential in the electrode/electrolyte interface, and the pres-

Table 2. RB5 Degradation parameters over different modified electrodes

Electrode	η/V	EF	% Discoloration at 120 min	k/min^{-1}
ME/Cu(15)-β	0.197	2.71	36	0.00376
ME/Cu(100)-β	0.212	0.42	27	0.00246
ME/Cu(15)-ZSM5	0.244	0.60	23	0.00194
ME/Cu(100)-ZSM5	0.208	1.4	30	0.00269

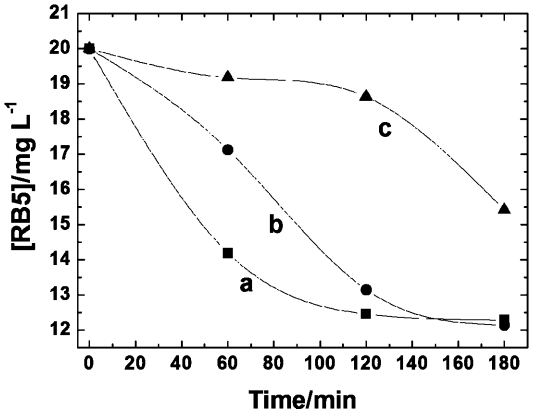

Figure 7. RB5 concentration in function of reaction time, reaction conditions: 3.3 g L^{-1} of H_2O_2 and NaCl (0.1 $molL^{-1}$), applied potentials at: a) -0.1, b) -0.05 and c) 0.05V/SCE.

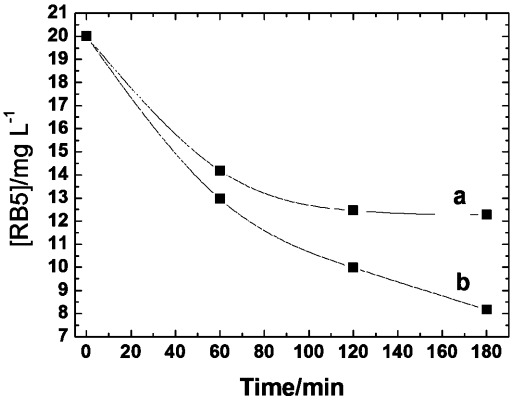

Figure 8. RB5 concentration in function of reaction time at -0.03 V/SCE, reaction conditions were: 3.3 g L^{-1} of H_2O_2 and NaCl (0.1 $molL^{-1}$), volume of dye solution: a) 5 mL and b) 2 mL.

ence of Cu^{2+} inhibits the HO formation according to the following reaction.

$$Cu^{2+} + H_2O_2 \rightarrow Cu^{+} + HO_2\bullet$$

On the other hand, when the applied potential was -0.1 V/SCE (curve a), the reaction occurred faster compared to -0.05 V/SCE (curve b). This occurs because when the applied potential is near to peak potential, kinetics electron transfer and diffusion control takes places, whereas at potential more cathodic (-0.1 V/SCE), the electrochemical process is controlled by diffusion. However, for both cathodic potential, the final discoloration efficiency was similar to 40%.

3.6. Electrode surface area and solution volume ratio Effect

In this study, it is clear that discoloration efficiency was relatively low. However, experiments were carried out using the microelectrolysis, where the relationship between dye solution volume and electrode surface area (V/A) was 25.5 mL cm^{-2} (Figure 8 curve a). In this context, experiments were performed to different V/A relationships; 10.2 mL cm^{-2} (Figure 8 curve b): the discoloration efficiency reached 60%, pointing out clearly that when the relationship V/A decreases, increasing the efficiency in the discoloration process.

4. CONCLUSION

This work, demonstrated that copper exchanged in Zeolite framework operates as a charge mediator for the electrocatalytic production of hydroxyl radical; this was verified by degradation of reactive black 5, which reduces its concentration in function of time; the best electrocatalytic activity was exhibited by ME/Cu- β with 15% of ionic exchange.

5. ACKNOWLEDGMENTS

CONACYT 101319 and SIP-IPN 20140793 projects, for financial support.

REFERENCES

[1] J.P. Aguer, F. Blachere, P. Boule, S. Garaudee, C. Guillard, Int. J. Photoenergy 2, 81 (2000).
[2] D.E. Kritiros, N.P. Xerouroulotaris, E. Psillaris, D. Mantzavinos, Water. Res. 41, 2236 (2007).
[3] C. Galindo, P. Jacques, A. Kalt, Chemosphere, 45, 997 (2001).
[4] A. Chen, X. Ma, H. Sun, J. Hazard. Mater., 156, 586 (2008).
[5] M.B. Kasiri, H. Aleboyeh, A. Aleboyeh, App. Catal. B: Environ., 84, 9 (2008).
[6] A. Aleboyeh, H. Aleboyeh, Y. Moussa, Dyes Pigments, 57, 67 (2003).
[7] P.R. Gogate, A.B. Pandit, Adv. Environ. Res., 8, 553 (2004).
[8] F.I. Hai, K. Yamamoto, K. Fukushi, Crit. Rev. Env. Sci. Technol., 37, 315 (2007).
[9] C. Minero, M. Lucchiari, D. Vione, V. Maurino, Env. Sci. Technol., 39, 8936, (2005).
[10] E. Brillas, M.A. Baños, S. Camps, C. Arias, P. Ll. Cabot, J.A. Garrido, R.M. Rodíguez, New. J. Chem., 28, 314 (2004).
[11] I. Melián-Cabrera, F. Kapteijn, J.A. Moulijn, Catal. Today, 110, 255 (2005).
[12] R. Gonzalez-Olmos, M.J. Martin, A. Georgi, F.D. Kopinke, I. Oller, S. Malato, Appl. Catal. B: Environ., 125, 51 (2012).
[13] K. Maduna Valkaj, A. Katovic, S. Zrnčević, J. Hazard. Mater., 144, 663 (2007).
[14] R. Gonzalez-Olmos, U. Roland, H. Toufar, F.-D. Kopinke, A. Georgi, Appl. Catal. B: Environ., 89, 356 (2009).
[15] M.A. Oliver-Tolentino, A. Guzmán-Vargas, E.M. Arce-Estrada, D. Ramírez-Rosales, A. Manzo-Robledo, E. Lima, J. Electroanal. Chem., 692, 31, (2013).
[16] A. Guzmán-Vargas, M.A. Oliver-Tolentino, E. Lima, J. Flores-Moreno, Electrohim. Acta, 108, 583 (2013).
[17] A. Guzmán-Vargas, G. Delahay, B. Coq, Appl. Catal. B: Environ., 42, 369 (2003).
[18] X. Ma, M. Zhou, J. Chem. Technol. Biotechnol., 84, 1544 (2009).